**Support information**

# Insights into the synergistic catalytic mechanism on the customized dual sites of an efficient ORR catalyst

Jinyu Zhao [a], Xu Chen [a], Jie Lian [a], Yu Gao [a], Yixing Zhang [a], Xiaomin Wang [a*]

[a] *College of Materials Science and Engineering, Taiyuan University of Technology, Taiyuan 030024, China;*

*E-mail address: wangxiaomin@tyut.edu.cn (X.Wang)*

**In-situ electrochemical Raman tests are as following:**

Integrating a custom cell for electrochemical test with Raman spectra to perform in situ tests, further collecting the intermediates signals on the surface of catalysts during ORR. The custom cell was a three-electrode system, and with CHI 760E for collecting electrochemical data. The glassy carbon electrode, with 4 times the area of the rotating ring disc electrode (RRDE), was the working electrode. This required that the catalyst ink be coated four times as much as for the ex-situ tests, thus ensuring that the in-situ Raman signals were captured. The Ag/AgCl (in saturated KCl), and Pt wire were reference and counter electrodes, respectively. The Raman light source with λ = 532 passed vertically through the window (quartz sheet) into the reaction cell to probe the sample surface. The acquisition time of the laser was 40 s, with the acquisition range of 0-2000 $cm^{-1}$. Each Raman spectrum was acquired at a constant voltage in the range of 1.05 V-0.15 V at 0.1 V intervals, while in-situ cyclic voltammetry (CV) test was performed in 0.5 M $H_2SO_4$ ($O_2$-saturated) at a very slow scan rate.

**All electrochemistry-related calculation equations are listed below：**

The electrochemical surface area ($ECSA_{Hupd}$) of the catalyst based on the hydrogen underpotential deposition ($H_{upd}$) peak is via **Eq. S1**,[1] as follow:

$$ECSA_{(Hupd)}\,(m^2\,g^{-1}) = \frac{\frac{S}{V}}{m_{Pt} \times 2.1(C\,m^{-2})}$$

Where S is the $H_{upd}$ integrated area from the CV curve. V is the scanning rate of 50 mV $s^{-1}$. $m_{Pt}$ is the actual Pt mass loadings on the WE. 2.1 is the number of charges adsorbed by Pt/unit area.

The kinetic current density ($J_k$) of the catalyst and the corresponding electron transfer number (n) are obtained through **Eq. S2** (namely, Koutecky-Levich, K-L),[2, 3] as follow:

$$\frac{1}{J} = \frac{1}{J_L} + \frac{1}{J_K} = \frac{1}{\frac{B}{\omega^{1/2}}} + \frac{1}{J_K}$$

$$B = 0.2nFC_0D_0^{2/3}\,\nu^{-1/6}$$

$$J_K = nFkC_0$$

Where J, $J_K$, and $J_L$ are the measured, kinetic, and limiting current densities, respectively. ω (rad $s^{-1}$) is the angular velocity. n is electron transfer number. F is the Faraday constant (96 485 C $mol^{-1}$). $C_0$ is the $O_2$ concentration (0.5 M $H_2SO_4$) and $D_0$ is the diffusion coefficient. ν is the electrolyte kinetic viscosity. $k$ is the constant of electron transfer rate.

The mass activity (MA) and specific activity (SA) of the catalyst are calculated by the following **Eq. S3** and **Eq. S4**[4, 5]:

$$MA = \frac{J_K}{m_{Pt}}$$

$$SA = \frac{J_K}{ECSA \times m_{Pt}}$$

Where $J_K$ is kinetic current density, $m_{Pt}$ is the actual Pt mass loadings on the WE. ECSA is the electrochemical surface area.

The electron transfer number ($n_{RRDE}$) from RRDE electrode and the $H_2O_2$ yield derive from the following **Eq. S5** and **Eq. S6**[6, 7]:

$$n_{RRDE} = \frac{4I_d}{I_d + \frac{I_r}{N}}$$

$$H_2O_2(\%) = 200 \times \frac{\frac{I_r}{N}}{\frac{I_r}{N} + I_d}$$

Where $I_d$ and $I_r$ are the disk and ring currents, respectively. N is the current collection efficiency of 0.37 from Pt ring.

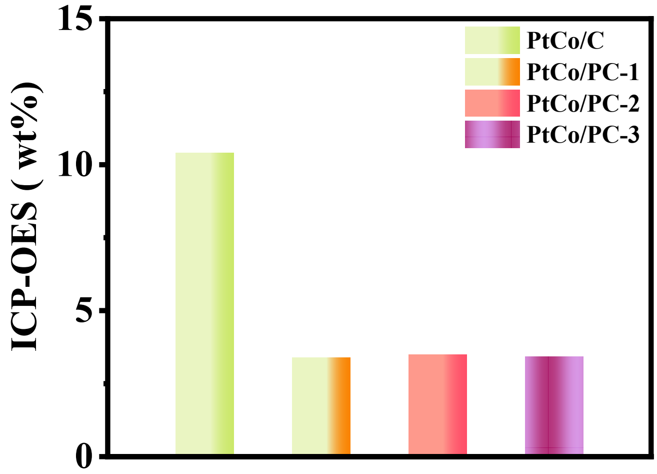


**Figure S1.** ICP statistical graph of PtCo/C, PtCo/PC-1, PtCo/PC-2, PtCo/PC-3.

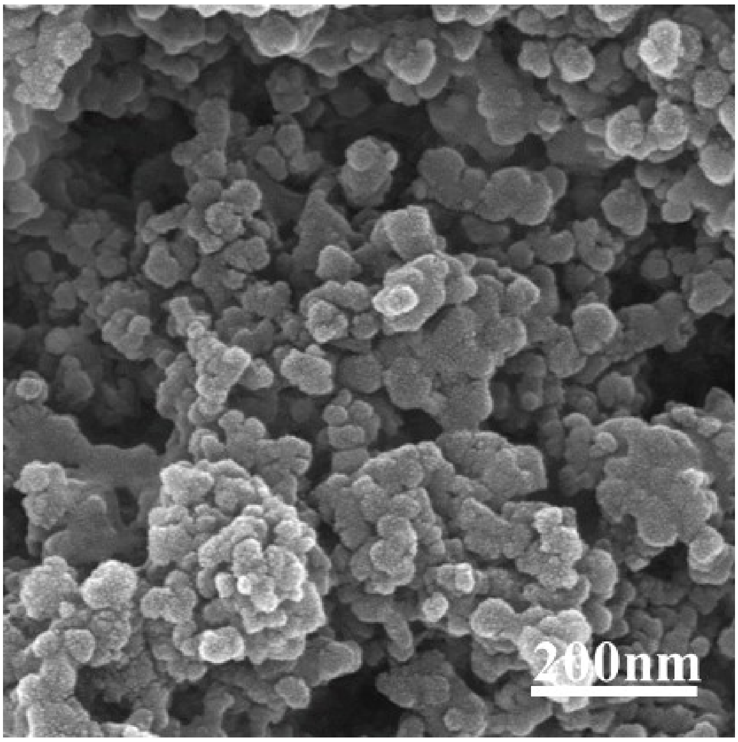


**Figure S2.** SEM image of PtCo/PC-2.

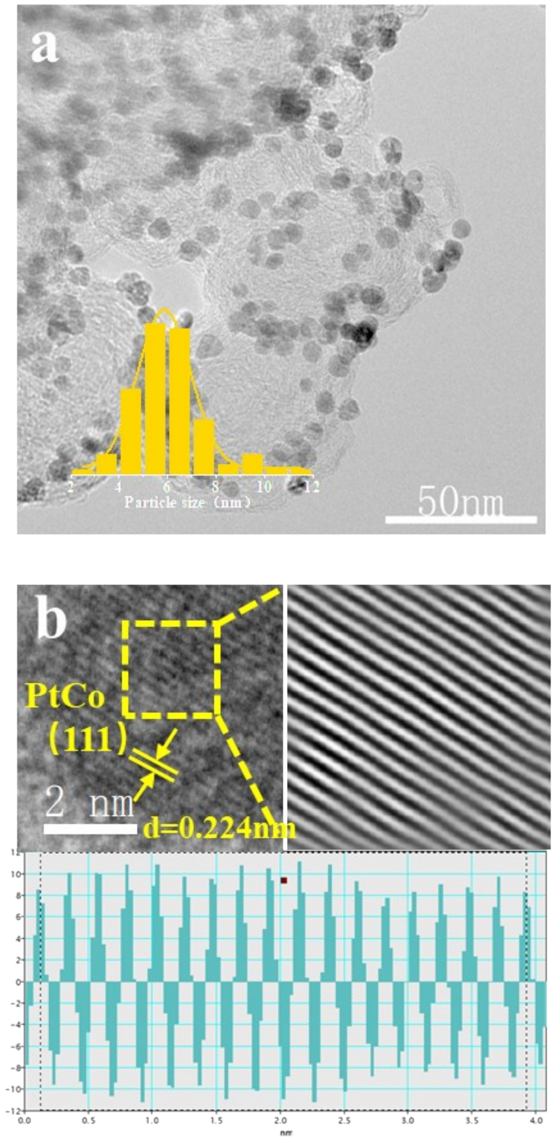


**Figure S3. (a)** The TEM image with particle size statistical histogram, **(c)** the HRTEM images with IFFT images and selected stripes histograms, all for PtCo/C.

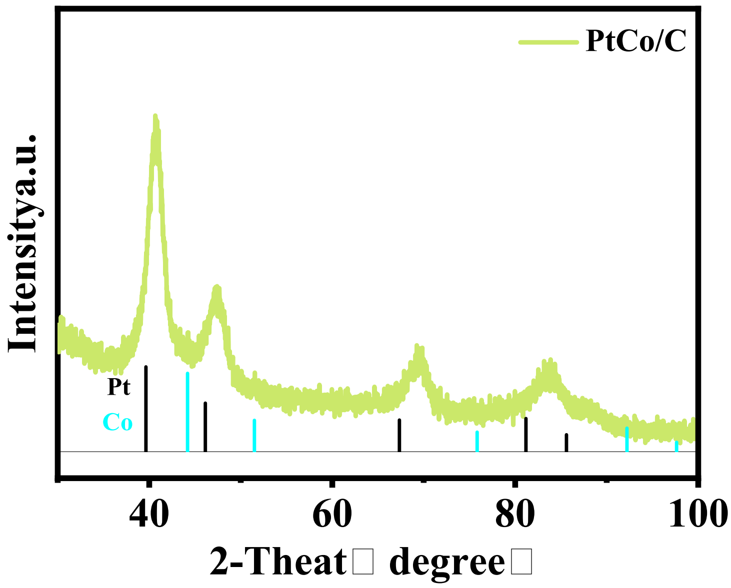


**Figure S4.** The XRD patterns of PtCo/C.

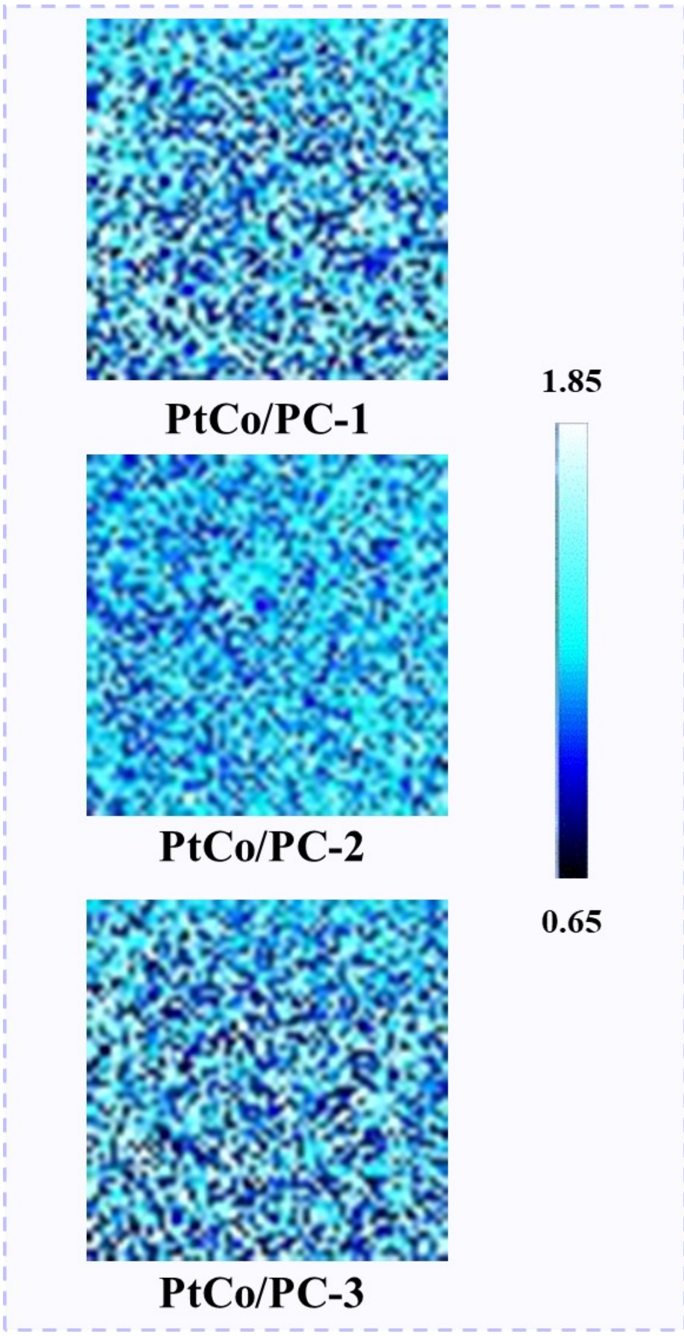


**Figure S5.** The Raman mapping map of $I_D/I_G$ in the 60 × 60 $um^2$ region for PtCo/PC-1, PtCo/PC-2, PtCo/PC-3.

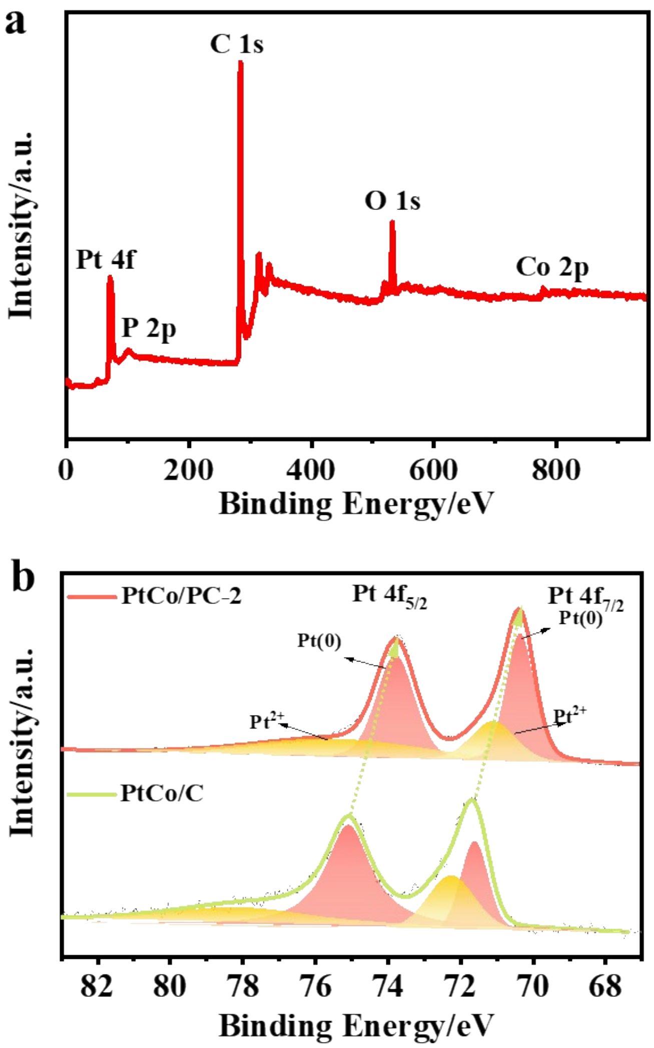


**Figure S6. (a)** The XPS survey scan of PtCo/PC-2. **(b)** The high resolution XPS spectra of Pt 4f for PtCo/C and PtCo/PC-2.

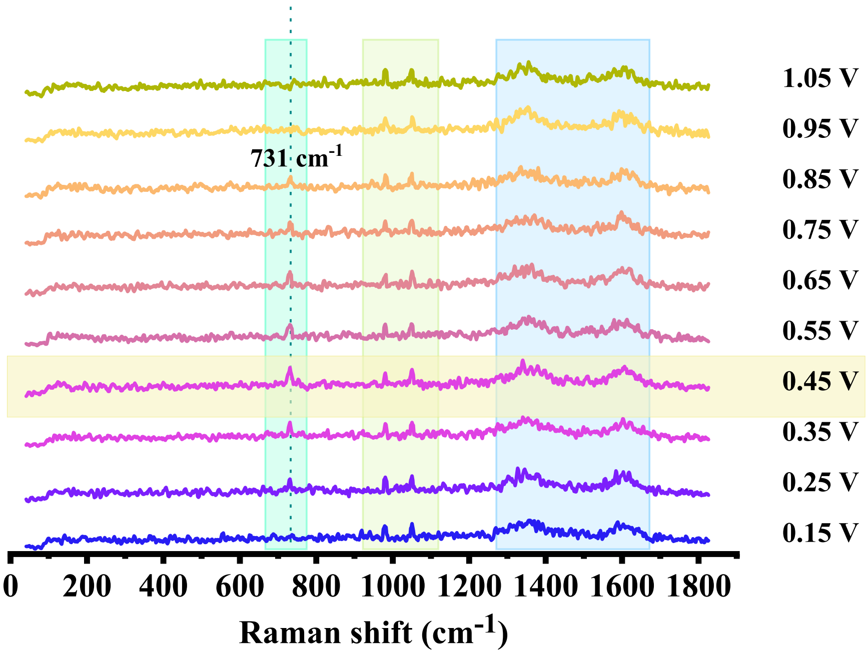


**Figure S7.** In-situ Raman spectra of intermediates on the surfaces for PtCo/C in $O_2$-saturated 0.5M $H_2SO_4$ (ORR) at different constant potentials.

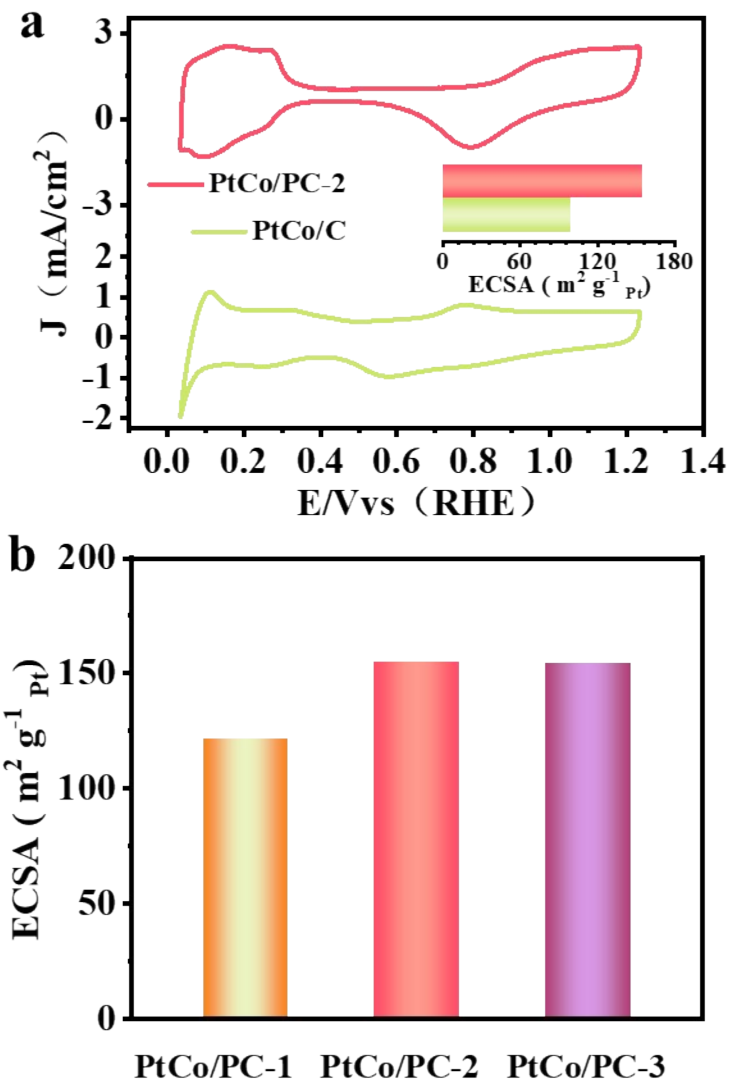


**Figure S8.** **(a)** CV curves of PtCo/PC-2 and PtCo/C, with the statistical histograms of $ECSA_{Hupd}$. **(b)** The statistical histograms of $ECSA_{Hupd}$ for PtCo/PC-1, PtCo/PC-2, PtCo/PC-3, all in $O_2$-saturated 0.5M $H_2SO_4$ (ORR).

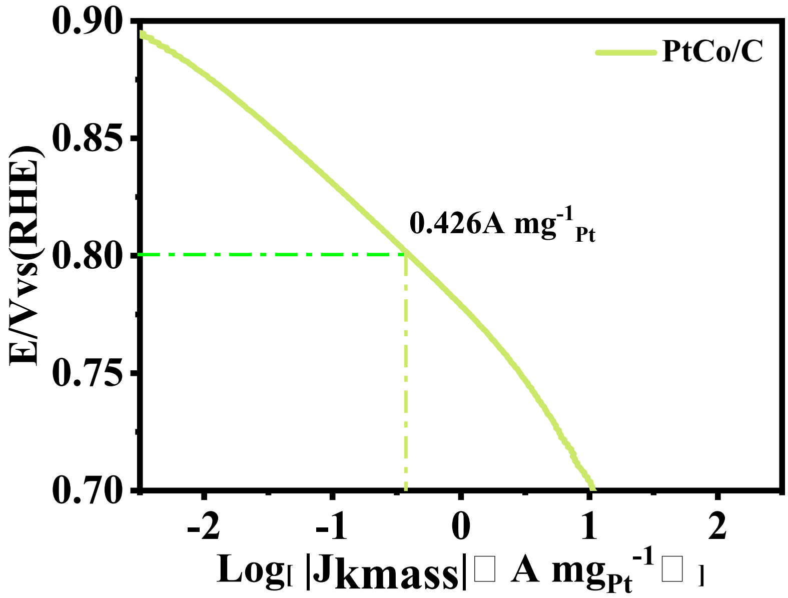


**Figure S9. (a)** MA curve of PtCo/C in $O_2$-saturated 0.5 M $H_2SO_4$ (ORR).

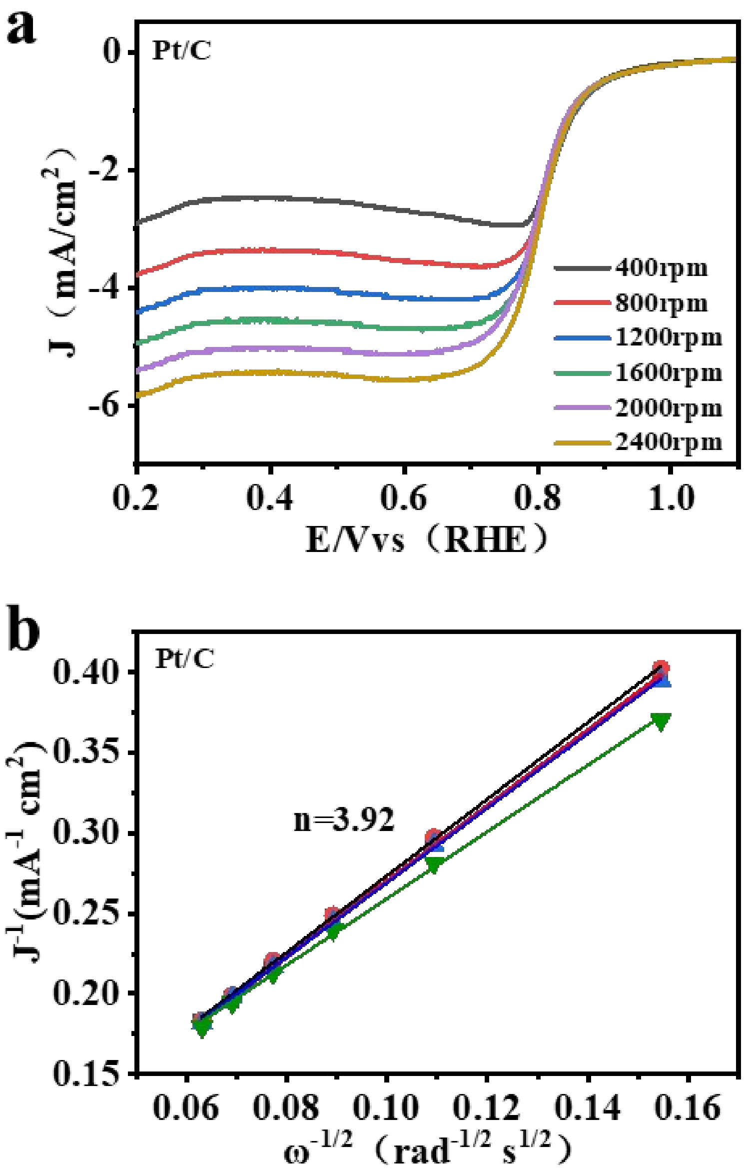


**Figure S10. (a)** LSV curves at different speeds of Pt/C, and **(b)** the corresponding K-L curves, all in $O_2$-saturated 0.5 M $H_2SO_4$ (ORR).

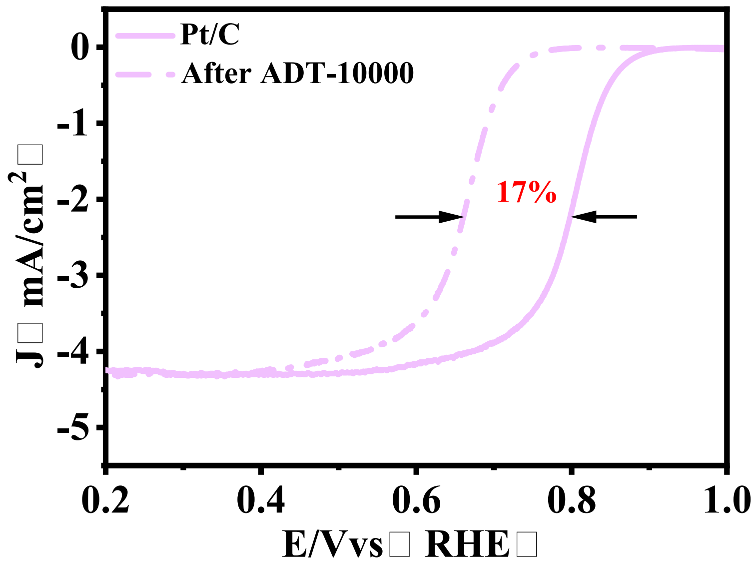


**Figure S11.** LSV curves of Pt/C at 1600 rpm before and after 10000s ADT in $O_2$-saturated 0.5 M $H_2SO_4$ (ORR).

## 【Reference】


1. W. Yun-Feng, M. Ji-Wei and H. Yun-Hui, *Rare Metals*, 2022, DOI: 10.1007/s12598-022-02119-6.
2. L. Yifei, P. Lishan, W. Chaoling, Y. Yigang, X. Haijiao, C. Yungui and W. Yao, *Nano Research*, 2023, DOI: 10.1007/s12274-023-5399-2.
3. J. Cao, H. Cao, F. Wang and H. Zhu, *Journal of Power Sources*, 2021, **489**.
4. S. He, Y. Liu, H. Zhan and L. Guan, *ACS Catalysis*, 2021, **11**, 9355-9365.
5. X. Li, J. Xi, L. Tang, H. Wang, Y. Liu, C. Min, S. Gao, F. Liu and X. Yang, *Electrochimica Acta*, 2023, **462**.
6. C. Zhang, Y. Dai, H. Chen, Y. Ma, B. Jing, Z. Cai, Y. Duan, B. Tang and J. Zou, *Journal of Materials Chemistry A*, 2018, DOI: 10.1039/c8ta08285e.
7. Y. Wu, Y. Zhao, J. Liu and F. Wang, *Journal of Materials Chemistry A*, 2018, DOI: 10.1039/c8ta00029h.